

# Toughening CO<sub>2</sub>-Derived Copolymer Elastomers Through Ionomer Networking

Kam C. Poon, Georgina L. Gregory, Gregory S. Sulley, Fernando Vidal, and Charlotte K. Williams\*

Utilizing carbon dioxide (CO<sub>2</sub>) to make polycarbonates through the ring-opening copolymerization (ROCOP) of CO<sub>2</sub> and epoxides valorizes and recycles CO<sub>2</sub> and reduces pollution in polymer manufacturing. Recent developments in catalysis provide access to polycarbonates with well-defined structures and allow for copolymerization with biomass-derived monomers; however, the resulting material properties are underinvestigated. Here, new types of CO<sub>2</sub>-derived thermoplastic elastomers (TPEs) are described together with a generally applicable method to augment tensile mechanical strength and Young's modulus without requiring material re-design. These TPEs combine high glass transition temperature ( $T_g$ ) amorphous blocks comprising CO<sub>2</sub>-derived poly(carbonates) (A-block), with low  $T_g$  poly( $\epsilon$ -decalactone), from castor oil, (B-block) in ABA structures. The poly(carbonate) blocks are selectively functionalized with metal-carboxylates where the metals are Na(I), Mg(II), Ca(II), Zn(II) and Al(III). The colorless polymers, featuring <1 wt% metal, show tunable thermal ( $T_g$ ), and mechanical (elongation at break, elasticity, creep-resistance) properties. The best elastomers show >50-fold higher Young's modulus and 21-times greater tensile strength, without compromise to elastic recovery, compared with the starting block polymers. They have wide operating temperatures (−20 to 200 °C), high creep-resistance and yet remain recyclable. In the future, these materials may substitute high-volume petrochemical elastomers and be utilized in high-growth fields like medicine, robotics, and electronics.

carbon dioxide (CO<sub>2</sub>) in combination with biomass. This could be important to tackle the ≈1.8 gigatonnes of CO<sub>2</sub>-equivalent (Gt-CO<sub>2</sub> equiv.) emitted annually from polymer production worldwide.<sup>[2]</sup> To accelerate change, these new polymer manufacturing and processing methods should be compatible with existing infrastructure and polymer properties must match or improve upon current products.<sup>[3]</sup> Once derived from renewable resources, materials must be designed for appropriate end-of-life re-use, low energy recycling and for safe disposal by complete degradation of the macromolecular structure.<sup>[4]</sup> There have been some tremendous advances in designing sustainable polymers but gaps remain in matching the property profile of current fossil-derived materials.<sup>[5]</sup>

Carbon dioxide is an attractive raw material as it is cheap, abundant, and a common waste product of chemical processes; its copolymerization with epoxides is a front-runner for carbon-capture and utilization (CCU) technology since it can be retro-fit into existing manufacturing plants and obviates the environmental trade-offs when biomass is used.<sup>[6]</sup>

Life-cycle analysis, comparing CO<sub>2</sub>-derived

polymers with polyethers (i.e., 100% epoxide) shows significant reductions in greenhouse gas emissions: for every CO<sub>2</sub> molecule polymerized, two further molecules are saved by replacing the epoxide.<sup>[7]</sup> Low-molar-mass, CO<sub>2</sub>-derived polyols are useful to make polyurethanes for flexible and rigid foams, elastomers, coatings and adhesives.<sup>[8]</sup> In contrast, high molar mass CO<sub>2</sub>-polycarbonates are less explored.<sup>[9]</sup> This discrepancy arises, in part, from challenges in polymerization catalysis and because many of these CO<sub>2</sub>-based thermoplastics are very brittle, with low elongations at break (e.g., <3% for poly(cyclohexene carbonate) and poly(limonene carbonate)).<sup>[10]</sup> The recently reported catalyzed depolymerization of high molar mass CO<sub>2</sub>-derived polycarbonates back to monomers, i.e., epoxides and CO<sub>2</sub>, offers a future chemical recycling route.<sup>[11]</sup> Higher molar mass CO<sub>2</sub>-derived polymers warrant materials development matching that given to polyols.

Thermoplastic elastomers (TPEs) are reprocessable alternatives to vulcanized rubber since they feature physical, rather than chemical, cross-linking, hence enabling efficient material

## 1. Introduction

Replacing petroleum-derived and environmentally persistent polymers with more sustainable alternatives is an urgent global challenge.<sup>[1]</sup> One option is to prepare polymers from recycled

K. C. Poon, G. L. Gregory, G. S. Sulley, F. Vidal, C. K. Williams  
Chemistry Research Laboratory  
Department of Chemistry  
University of Oxford  
Oxford OX1 3TA, UK  
E-mail: charlotte.williams@chem.ox.ac.uk

 The ORCID identification number(s) for the author(s) of this article can be found under <https://doi.org/10.1002/adma.202302825>

© 2023 The Authors. Advanced Materials published by Wiley-VCH GmbH. This is an open access article under the terms of the Creative Commons Attribution License, which permits use, distribution and reproduction in any medium, provided the original work is properly cited.

DOI: 10.1002/adma.202302825

recycling. They are industrially important in automotives (tubing, tyres), electronics (cables), apparel (shoe soles) and speciality products (sports equipment or medical devices).<sup>[12]</sup> Petrochemical TPEs are derived from a range of olefins including styrene, butadiene, ethene, octene, propene or acrylates.<sup>[13]</sup> Block polymer TPEs feature phase-separated ABA structures, where the A domains comprise rigid or glassy polymer blocks ( $T_g$  or  $T_m > \text{room temperature}$ ) and B domains, the majority phase, are elastomers ( $T_g$  and  $T_m < \text{room temperature}$ ). These block polymers typically feature  $\approx 20\text{--}30 \text{ wt\%}$  A-block compositions and have overall  $M_n > 60 \text{ kg mol}^{-1}$  resulting in microphase-separated body-centered-cubic or hexagonally packed cylindrical morphologies.<sup>[11,14]</sup>

The syntheses of the ABA block polyolefins requires careful control over monomer addition timing, macro-monomer purification and, in some case, very low temperatures with the associated energy inputs.<sup>[12,13]</sup> Alternative materials need straightforward polymer syntheses, ideally operating with a single catalyst and in one reactor. Switchable catalysis allows for exactly such chemistry by coupling epoxide/ $\text{CO}_2$  ring-opening copolymerization (ROCOP) with cyclic ester ring-opening polymerization (ROP), using a single catalyst and reactor process.<sup>[15]</sup> Previously, a  $[\text{Zn(II)Mg(II)}]$  heterodinuclear metal catalyst produced high molar mass ABA triblock copolymers, comprising  $\text{CO}_2$ -polycarbonate (A-block) and castor oil-derived poly( $\epsilon$ -decalactone) (B-block).<sup>[11,14,16]</sup> The catalysis was well-controlled and as the  $\text{CO}_2$  content was increased, the polymer properties varied from adhesives to low-strength elastomers to toughened plastics. An alternative approach by Wu et al. demonstrated a straightforward protocol to finely tune the mechanical properties of a  $\text{CO}_2$ -based polyurethane thermoset.<sup>[17]</sup> These materials were synthesized through the grafting of poly( $\gamma$ -methyl- $\epsilon$ -caprolactone) onto pendent alcohol groups decorating a poly(vinyl cyclohexene oxide-*co*-cyclohexene oxide) backbone, followed by isocyanate coupling.

In Nature, biopolymer–metal networks reinforce and toughen materials. Examples include peptide–iron–catechol complexes employed by marine mussels in byssal threads to adhere them to rocks in tidal regions;<sup>[18]</sup> zinc complexes that harden insect mandibles;<sup>[19]</sup> and calcium–polymer bonds that are integral to shells, bones and skeletons.<sup>[20]</sup> Here, metal–polymer coordination chemistry is applied as a means to moderate elastomer properties since both the binding energy (thermodynamics) and ligand-exchange lability (kinetics) are tunable. We hypothesized that from a common polymer precursor, elastomeric properties might be modified by changing both the metal and loading used. This strategy could be advantageous since it would eliminate the need for new monomers or for control over polymer crystallization, both aspects can be difficult to scale, control and may complicate recycling. In fact, commercial elastomer–metal networks are known, sometimes referred to as ionomers when low metal loadings are applied. For example, the TPE ionomer Surlyn is a random copolymer of ethylene and methacrylic acid reinforced with sodium ions and is used in food packaging. So far, commercial ionomers feature ill-defined polymer structures and so deconvoluting influences of metal coordination chemistry would be very challenging. Recently, the incorporation of metals into better-defined polymer matrices has drawn interest for their responsive luminescence, self-healing, catalytic and toughening potential.

Many of these materials have specific but limited applications, in part because of their intense colors.<sup>[21]</sup>

Well-defined polymer–metal complex interactions are much better understood in soft materials, like hydrogels, and have shown real promise in improving their properties.<sup>[22]</sup> There is much less investigation of their potential to moderate plastics or elastomers; material classes typically exhibiting 100–1000 times greater tensile strength and 10–100 000 times higher Young's modulus than gels. By applying strategies adopted in hydrogels, elastomers and plastics could have the potential for dramatic improvements in mechanical properties.<sup>[23]</sup> One example, from Valentine et al., demonstrated that incorporating iron–catechol interactions into a very low tensile strength polyether improved tensile strength and toughness.<sup>[24]</sup> In 2022, we reported ABA block polymer TPEs (A = polyester, B = polyester/carbonate) featuring sodium-, or zinc-carboxylate complexation in the hard domains that showed high tensile strengths and Young's moduli.<sup>[14b,c]</sup> The correlations between material properties and either the nature of or loading of different metals is under-explored.

In this work, a  $\text{CO}_2$ -derived polycarbonate, poly(vinyl-cyclohexene carbonate) (A-block), and bio-derived polyester, poly( $\epsilon$ -decalactone) (B-block), are combined in an ABA block copolymer, featuring carboxylic acids attached to each polycarbonate repeat unit. The polymer coordination chemistry is investigated with sodium(I), magnesium(II), calcium(II), zinc(II) or aluminum(III) as a strategy to reinforce A-block domains in thermoplastic elastomers. These metals are selected to be colorless, Earth-abundant, inexpensive, low-weight, low toxicity and to feature strong bonding to carboxylic acids. The goals are to discover methods to use metal complexation to moderate the TPE tensile strength, Young's modulus and toughness without compromising elastic recovery or recyclability.

## 2. Results

### 2.1. Polymer Syntheses

The ABA triblock copolymer, poly(vinyl-cyclohexene carbonate-*b*- $\epsilon$ -decalactone-*b*-vinyl-cyclohexene carbonate) (PvCHC-PDL-PvCHC) was prepared using switchable catalysis, in a one-pot process, with a heterodinuclear  $[\text{LZnMg}(\text{C}_6\text{F}_5)_2]$  catalyst and 1,4-benzenedimethanol (BDM), as both initiator and chain transfer agent (CTA) (Figure 1). Starting from a mixture of  $\epsilon$ -decalactone (DL) and 4-vinyl-cyclohexene oxide (vCHO), the  $[\text{Zn(II)Mg(II)}]$  metal catalyst first undergoes ring-opening polymerization (ROP) of DL, forming only a telechelic poly( $\epsilon$ -decalactone) (PDL B-block). Next, the reactor was pressurized with  $\text{CO}_2$  (20 bar), triggering the alternating ring-opening copolymerization (ROCOP) of  $\text{CO}_2$ /epoxide, and forming the desired ABA triblock copolymer (Figure S1, Supporting Information). The benefits of this highly selective and well-controlled catalytic system are that there is: (i) no need for any intermediate polymer isolation or purification, and (ii) production of monomodal, high molar mass polymers with high end-group fidelity ( $M_n > 50 \text{ kg mol}^{-1}$ ,  $D_M = 1.2$ ).<sup>[15a]</sup> As an example of how this reaction was conducted, DL, vCHO, BDM and  $[\text{LZnMg}(\text{C}_6\text{F}_5)_2]$  catalyst were dissolved in toluene and reacted at  $80^\circ\text{C}$ , for 120 min ( $[\text{LZnMg}(\text{C}_6\text{F}_5)_2]_0 = 1.0 \text{ mM}$ ,  $[\text{LZnMg}(\text{C}_6\text{F}_5)_2]:[\text{BDM}]:[\text{vCHO}]:[\text{DL}] = 1:4:938:1645$ ). The ROP of DL occurred in high conversion to form the

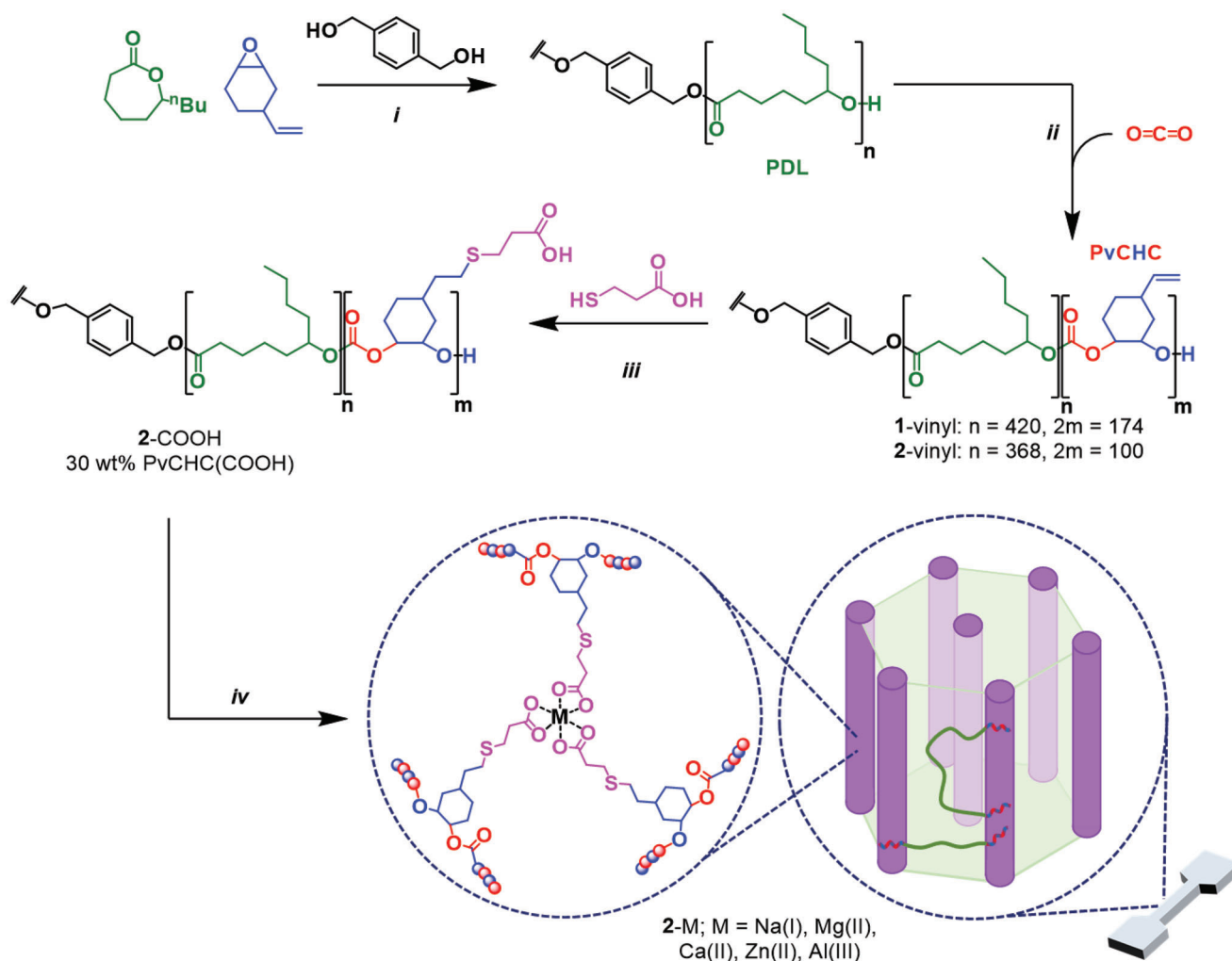


**Figure 1.** Synthesis of poly(carbonate-*b*-ester-*b*-carbonate) ionomers. i) DL ROP at 80 °C catalyzed by [LZnMg(C<sub>6</sub>F<sub>5</sub>)<sub>2</sub>] with BDM as a bifunctional initiator, where [Cat]<sub>0</sub>: [BDM]<sub>0</sub>: [ε-DL]<sub>0</sub> = 1:4:1644 (1-vinyl), [ε-DL]<sub>0</sub> = 1.7 M, toluene; ii) CO<sub>2</sub>/vCHO ROCOP, CO<sub>2</sub> (20 bar), 80 °C. PvCHC-PDL-PvCHC (1-vinyl):  $M_{n,SEC} = 97 \text{ kg mol}^{-1}$  ( $\bar{D}_M = 1.09$ ), 29 wt% PvCHC by <sup>1</sup>H NMR spectroscopy. 2-Vinyl:  $M_{n,SEC} = 67 \text{ kg mol}^{-1}$  ( $\bar{D}_M = 1.12$ ), 21 wt% PvCHC; iii) carboxylic acid functionalization (rt, 1 h) with 3-mercaptopropionic (3-MPA) and DMPA photoinitiator, 365 nm. [2-vinyl] = 5 wt%, THF. For P<sub>COOH</sub>CHC-PDL-P<sub>COOH</sub>CHC (2-COOH), 30 wt% P<sub>COOH</sub>CHC. iv) Coordination of Na(I), Mg(II), Ca(II), Zn(II) and Al(III). [2-COOH] = 5 wt%, THF. [COOH]<sub>0</sub>: [M]<sub>0</sub> = 10:1 for all metals. 50 mM stock solutions of NaOTf, Al(OTf)<sub>3</sub> in THF and Mg(OTf)<sub>2</sub>, Ca(OTf)<sub>2</sub>, Zn(OTf)<sub>2</sub> in H<sub>2</sub>O used to add desired quantity of metals.

PDL block (90%, TOF = 740 h<sup>-1</sup>), as confirmed by <sup>1</sup>H NMR spectroscopy from a reaction aliquot (Table S1, Supporting Information). Then, the reaction mixture was transferred into a steel Parr reactor, the atmosphere was replaced with CO<sub>2</sub> (20 bar) and heated to 80 °C to switch to the efficient ROCOP of vCHO/CO<sub>2</sub>. After stirring for 48 h, the reactor was cooled and depressurized, at which point analysis by <sup>1</sup>H NMR spectroscopy indicated 84% conversion to the desired PvCHC “hard” blocks (>99% CO<sub>2</sub> selectivity, >99% polymer selectivity, TOF = 13 h<sup>-1</sup>). Further analysis by <sup>1</sup>H NMR spectroscopy, of the isolated material, after precipitation in MeOH, established it comprised 29 wt.% PvCHC (A-block). This value was deduced by comparing integrals of resonances at 2.27 ppm (PDL main-chain -CH<sub>2</sub>-) and 5.76 ppm (PvCHC -CH = CH<sub>2</sub>) (Figure S2, Supporting Information). The polymer, 1-vinyl, showed a high molar mass (number average molecular weight,  $M_n = 97 \text{ kg mol}^{-1}$ ) and narrow dispersity

( $\bar{D}_M = 1.09$ ), as determined by size-exclusion chromatography, SEC (Figure S5, Supporting Information). The desired ABA triblock copolymer structure was confirmed by analysis of chain end-groups, by <sup>31</sup>P{<sup>1</sup>H} NMR spectroscopy after treatment with a phospholane reagent, which showed the exclusive formation of hydroxyl telechelic polymers originating from the outer PvCHC (A-block) (Figure S6, Supporting Information).<sup>[25]</sup> Also, 2D DOSY NMR spectroscopy displayed a single diffusion coefficient for all signals consistent with the block copolymer structure (Figure S7, Supporting Information).

Next, carboxylic acids were installed onto every polycarbonate repeat by using a UV-initiated “thiol-ene” reaction between the polymer vinyl substituents and 3-mercaptopropionic acid (3-MPA). To allow for proper comparison between equivalent “unfunctionalized” and ionomeric elastomers, a constant polycarbonate (A-block) weight fraction (%) was used for all polymers

**Table 1.** ABA triblock characterization data.

Polymer	DP PvCHC:PDL:PvCHC <sup>a)</sup>	wt% hard block <sup>a)</sup>	$M_{n,NMR}$ <sup>a)</sup> [kg mol <sup>-1</sup> ]	$M_{n,SEC}$ <sup>b)</sup> [kg mol <sup>-1</sup> ]	$\bar{D}_M$ <sup>c)</sup>	Classification
1-vinyl	87:420:87	29	100.7	96.7	1.09	Elastomer
2-vinyl	50:368:50	21	79.4	67.3	1.12	Viscoelastic liquid
2-COOH	50:368:50	30	106.6	43.0	1.45	Elastomer

<sup>a)</sup> Determined from <sup>1</sup>H NMR spectrum of purified samples (Figure S2, Supporting Information); <sup>b)</sup> Determined from SEC analysis (THF, 1 mL min<sup>-1</sup>); calibrated with narrow poly(styrene) standards (Figures S5 and S10, Supporting Information); <sup>c)</sup>  $M_w/M_n$ .

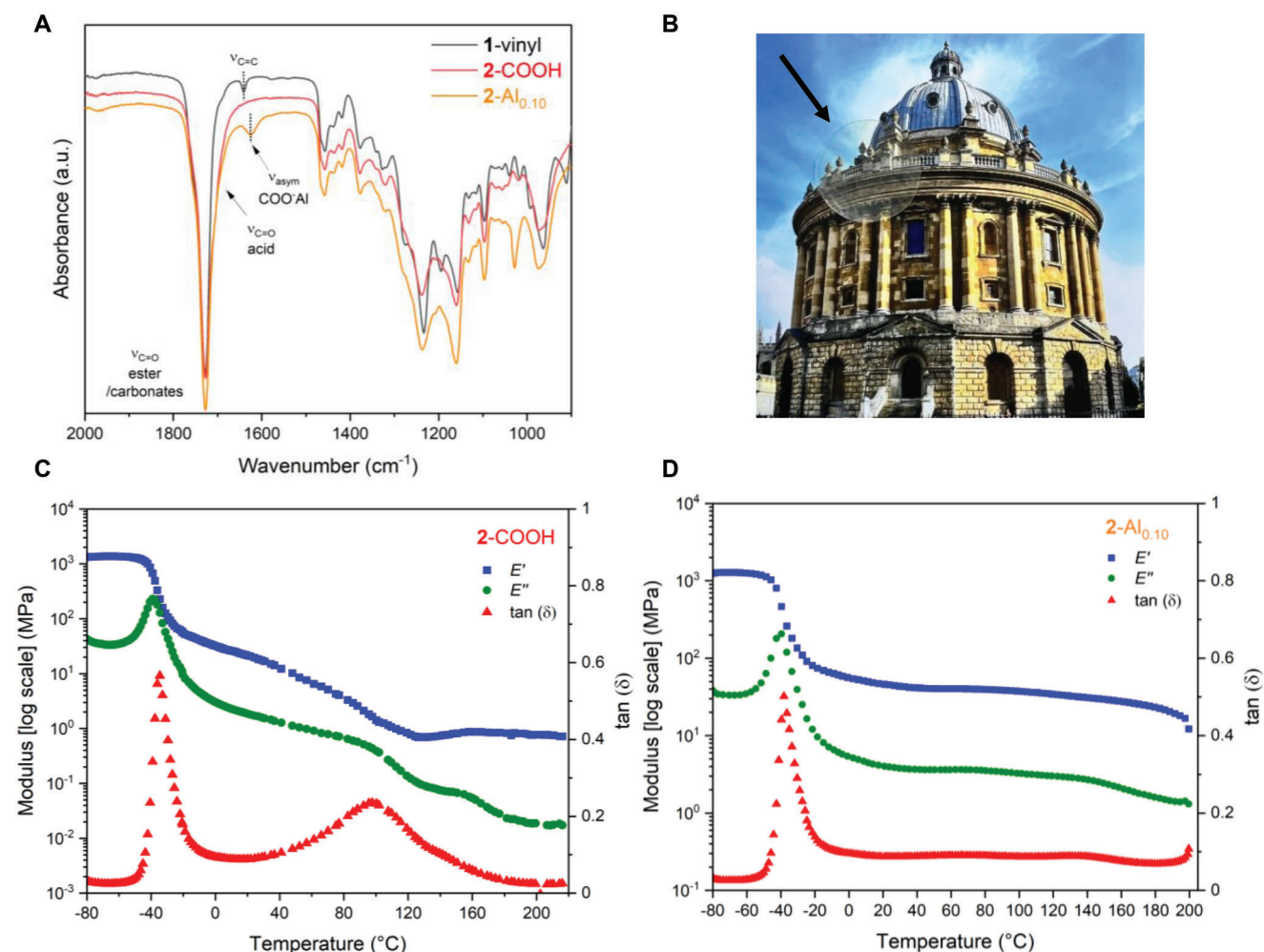


**Figure 2.** Characterization of CO<sub>2</sub>-derived triblock copolymer elastomers. A) FTIR spectra of polymer films comparing the unfunctionalized (1-vinyl), carboxylic acid functionalized (2-COOH) and aluminum ionomer (2-Al<sub>0.10</sub>) materials. B) Photograph showing the transparent film of 2-Al<sub>0.10</sub> superimposed upon a colored background. C,D) Dynamic mechanical thermal analysis (DMTA) temperature sweeps for the carboxylic acid functionalized (2-COOH) (C) and the aluminum ionomer (2-Al<sub>0.10</sub>) (D) materials.

(Table 1). Accordingly, a second unfunctionalized block polymer featuring a lower (21 wt%) polycarbonate content was synthesized (2-vinyl), with this material delivering 30 wt% polycarbonate after carboxylic acid installation (2-COOH).

Quantitative carboxylic acid functionalization was confirmed using <sup>1</sup>H NMR spectroscopy, which showed the disappearance of the vinyl resonances and the appearance of three new signals for the carboxylic acids (Figure S8, Supporting Information). The <sup>13</sup>C{<sup>1</sup>H} NMR spectra confirmed complete consumption of

the vinyl signals (114, 142 ppm) and formation of a new carboxylic acid signal (177 ppm) without changes to polymer carbonate resonances (153 ppm, Figure S9, Supporting Information). The IR spectra showed the disappearance of the vinyl resonance (1641 cm<sup>-1</sup>) and the appearance of a broad carbonyl resonance (1728 cm<sup>-1</sup>, Figure 2a). SEC analyses revealed a slight decrease in the overall polymer molar mass after functionalization, but with retention of a monomodal distribution (2-COOH, Figure S10, Supporting Information). The decrease in molar



mass is likely an SEC artefact since the carboxylic acids are expected to significantly change the polymers' hydrodynamic radius. By reacting the pendant carboxylic acid groups with an excess of 2-chloro-4,4,5,5-tetramethyl dioxaphospholane the inter-chain hydrogen bonding was disrupted and the SEC trace of the resulting "masked" polymer sample revealed an increase in average molar mass and narrowing of dispersity compared with 2-vinyl (Figure S10, Supporting Information). The  $M_{n,NMR}$  also showed the expected increase in molar mass after functionalization. There was no evidence for any backbone degradation or vinyl crosslinking, by either NMR or SEC analyses. The  $^1H$  DOSY NMR spectrum showed a single diffusion coefficient consistent with the polymer structure (Figure S11, Supporting Information). There was also a significant change in material properties, with 2-vinyl behaving as a viscoelastic liquid, while 2-COOH is an elastomeric solid (Figure S12, Supporting Information).

From 2-COOH, a series of metal complex ionomers were synthesized using sodium(I), magnesium(II), calcium(II), zinc(II) and aluminum(III). These metals were selected based on Earth-abundance, low cost, low weight, and lack of color as well as for their strong precedent for reacting with carboxylic acids. By using mono-, di- and trivalent metals it is possible to compare the influences of metal ionic radii and coordination chemistries on the elastomer properties. All ionomer syntheses were scalable within the laboratory; thus, 10.4 g of 2-vinyl was transformed into 9.0 g of 2-COOH that was used for all subsequent metal complexation reactions. To investigate the influences of the different metals, a common molar ratio of (Polymer)-COOH: metal, 10 : 1 was targeted, i.e., 10, 20 or 30% metal-carboxylate formation depending upon the valency of the metal. The ionomers were each synthesized by stirring a solution of 2-COOH (5 wt% in THF) with the appropriate metal triflate salt (a 50 mM solution of NaOTf, Al(OTf)<sub>3</sub> in THF, or Mg(OTf)<sub>2</sub>, Ca(OTf)<sub>2</sub>, Zn(OTf)<sub>2</sub> in H<sub>2</sub>O) for 10 min, at room temperature. Triflate salts were employed due to their favorable solubility in organic solvents, weakly coordinating anion and to maintain a consistent synthetic protocol, allowing for fair comparisons between the ionomers. The products were precipitated (methanol), washed with water to remove any released triflic acid, dried under reduced pressure and compression moulded into thin films (120 °C, 1 tonne, 10 min). The resulting films had variable but low metal weight contents (0.3–0.8 wt% overall) and consistent metal mol%.

The samples are henceforth referred to as 2-M<sub>x,xx</sub>, (M = metal employed, x.xx = metal loading relative to COOH groups). Formation of the (–COO)<sub>x</sub>M moieties (x = 1, 2, or 3) in the final film was supported by a range of spectroscopic techniques. FTIR spectroscopy confirms the metal-carboxylate coordination as exemplified by 2-Al<sub>0.10</sub> showed a clear peak at 1627 cm<sup>–1</sup> consistent with metal carboxylate formation (Figure 2a; Figures S13–S19, Supporting Information).<sup>[14b,23f,26]</sup> All the ionomer films were optically transparent as confirmed by UV–vis spectra (Figure 2b; Figures S20–S28, Supporting Information). Coordination of Al(III) to the carboxylate ligands was also confirmed by solid-state <sup>27</sup>Al NMR spectroscopy using a film of 2-Al<sub>0.10</sub> (Figure S29, Supporting Information). Signals at 182 and –202 ppm, which arise from <sup>27</sup>Al-<sup>19</sup>F coupling in Al(OTf)<sub>3</sub> disappeared, consistent with the loss of triflate anions, and a new broad singlet at –6 ppm suggests there is a single aluminum coordination environment within the ionomer network.

## 2.2. Polymer Properties

### 2.2.1. Thermal Properties

The polymers were all amorphous with phase-separated microstructures, as determined by differential scanning calorimetry (DSC). Indeed, the two glass transition temperatures ( $T_g$ ) observed in the DSC thermograms are consistent with the values observed for the constituent polymer blocks (Figure S30, Supporting Information). The lower glass transition temperature ( $-46 \leq T_g \leq -54$  °C) corresponds to the PDL block. Interestingly, samples with 2-COOH and 2-M<sub>x,xx</sub> displayed slightly lower values, in both DSC and dynamic mechanical analyses (DMTA) profiles, likely due to greater block incompatibility between the non-polar PDL and more hydrophilic hard-blocks. The upper glass transition temperature, corresponding to the hard-blocks, was only detected by DSC for the unfunctionalized 1-vinyl ( $T_g = 105$  °C). A better insight into the thermal transition of the PvCHC functionalized A-block domains was obtained by DMTA. Thus, thin films of 2-COOH, 2-Na<sub>0.10</sub>, 2-Mg<sub>0.10</sub>, 2-Ca<sub>0.10</sub> and 2-Zn<sub>0.10</sub> displayed distinct peaks in their tan( $\delta$ ) profile (80–100 °C, Figure 2c; Figures S31–S37, Supporting Information), a clear indicator of the hard block  $T_g$ . For 2-Al<sub>0.10</sub>, a low-intensity, diffuse peak at a significantly higher temperature (136 °C) was attributed to greater cross-link density afforded by the trivalent metal that restricts chain segmental motion. This property provides the material with an extended rubbery plateau compared to the other ionomers spanning, from –20 to 200 °C, over that range the material maintained its constant storage modulus. Finally, the high thermal stability, as determined by thermogravimetric analysis ( $T_{d,5\%} > 250$  °C), indicates a wide processing window for all polymers (Figures S38–S47, Supporting Information).

### 2.2.2. Small-Angle X-ray Scattering

To better understand the block polymer morphologies, small-angle X-ray scattering (SAXS) was conducted on all films, at room temperature. No pre-treatment was conducted to better reflect the "true morphology" of samples used in subsequent mechanical testing (Table S3 and Figures S49–S54, Supporting Information). All polymers exhibit hexagonally packed cylindrical morphologies, as indicated by common higher-order scattering peaks ( $q/q^* = \sqrt{3}, \sqrt{4}, \sqrt{7}$  and  $\sqrt{9}$ ). This finding is important since it allows for comparisons of the metal influences without altering their phase-separated microstructures. The domain sizes ( $d = 2\pi/q^*$ ), determined from the principle scattering peaks ( $q^*$ ), increased slightly after functionalization from 15 nm for 1-vinyl to 21 and 20 nm for 2-COOH and 2-Al<sub>0.10</sub>, respectively (Figure 3a). All the ionomers have domain sizes between 20 and 27 nm. This increase in domain spacing upon functionalization is consistent with both carboxylic acid hydrogen bonding and metal–ligand coordination interactions within the hard domains.

### 2.2.3. Mechanical Properties

To study how the mechanical properties changed with metal-carboxylate coordination chemistry and to assess the stress–strain relationships of the thermoplastic elastomers, specimens

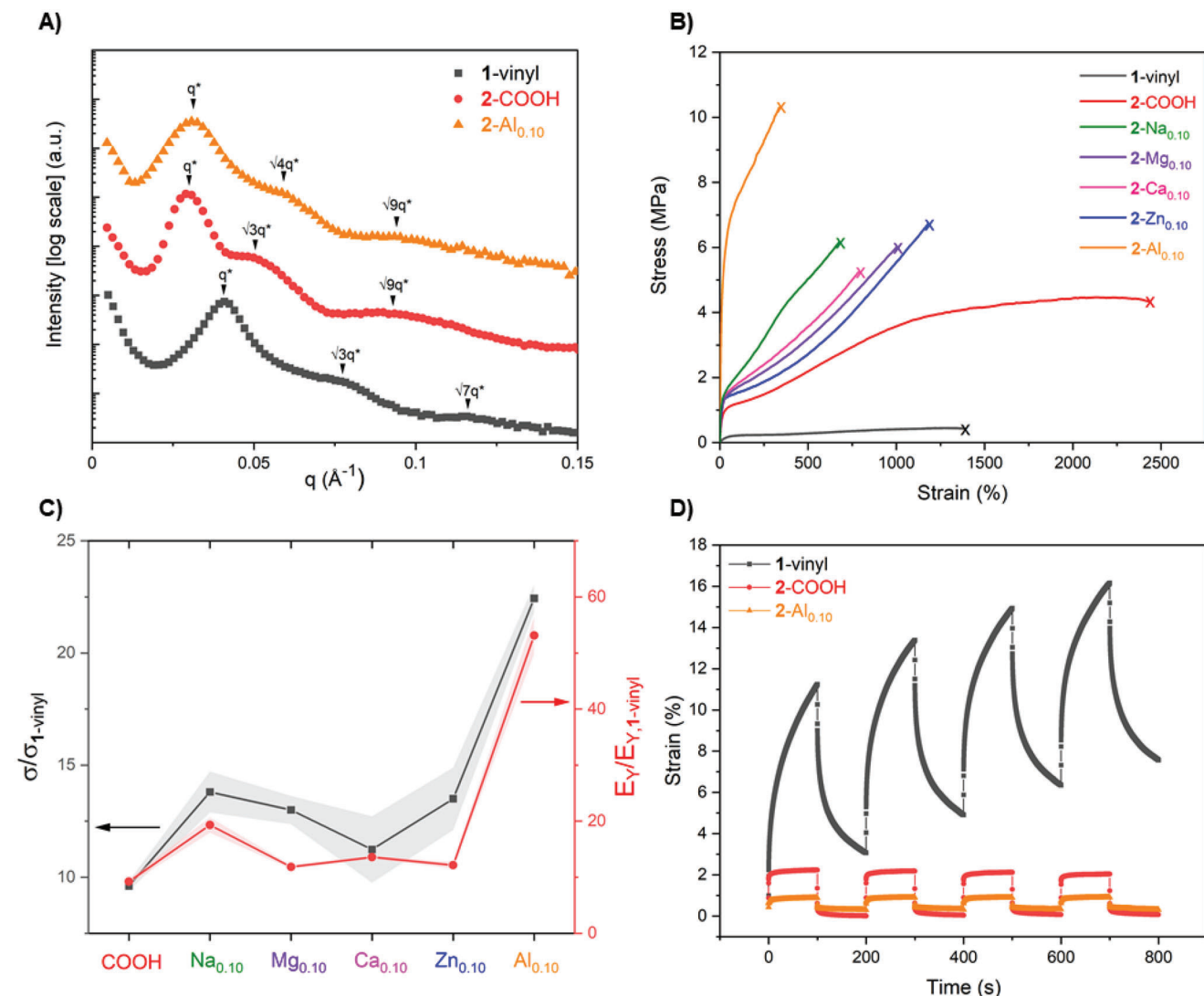


**Figure 3.** SAXS and mechanical properties of CO<sub>2</sub>-derived triblock copolymer elastomers. A) Room-temperature small-angle X-ray scattering (SAXS) profiles showing principle scattering peaks ( $q^*$ ) and higher-order peaks ( $q/q^*$ ). B) Representative stress–strain curves (10 mm min<sup>-1</sup> extension rate). C) Improvement in tensile strength and Young's modulus relative to unfunctionalized 1-vinyl. D) Creep–recovery experiments at 30 °C, 5 kPa.

were subjected to uniaxial extension experiments, according to ISO 527 (10 mm min<sup>-1</sup>) (Figure 3b). It was anticipated that a range of mechanical properties would be accessed by changing the valency and ionic radii of the metals. For each material, five repeat experiments were conducted, and the average values and errors, for the Young's modulus, tensile strength, strain at break and tensile toughness were compared (Table 2).

Samples showed tensile strengths from 1–10 MPa and elongations at break from 300%–2600%. All samples show stress–strain relationships, consistent with elastomeric behavior. The unfunctionalized polymer 1-vinyl shows a very low tensile strength, 0.5 MPa, and high elongation at break (1373%). There are clear material property benefits to the carboxylic acid functionalization in improving mechanical performance. Comparing materials with identical hard block content, 1-vinyl (unfunctionalized) and 2-COOH, reveals a 9-fold increase in Young's modulus (1.0 to 9.0 MPa), a 10-fold increase in tensile strength (0.5 to 4.4 MPa),

a 2-fold increase in elongation at break (1373 to 2615%), and a 19-fold increase in tensile toughness (4.7 to 88.4 MJ m<sup>-3</sup>). These superior properties are attributed to enhanced phase separation and the hydrogen bonding reinforcing the hard block. The mechanical properties were also significantly influenced by the different metals (Figure 3b). All displayed superior characteristics relative to 1-vinyl and 2-COOH, albeit with very high elongations at break (<1200%). Interestingly, monovalent 2-Na<sub>0.10</sub> displayed the greatest Young's modulus and tensile strength relative to all the metal(I) and metal(II) ionomers studied, which was tentatively attributed to the sodium carboxylate clustering/aggregation in the hard domains.

2-Al<sub>0.10</sub> shows the most dramatic increase in tensile strength (52-fold) and Young's modulus (21-fold) relative to the unfunctionalized triblock copolymer. The trivalent Al(III) ions enable greater cross-linking that reinforces the hard domains and strengthens the material. The gains in stiffness and strength

**Table 2.** Summary of thermal and mechanical properties of CO<sub>2</sub>-derived triblock copolymer elastomers.

Polymer	Metal [wt%]	<sup>a)</sup> $T_{g1}$ [°C]	<sup>b)</sup> $T_{g2}$ [°C]	<sup>c)</sup> $T_{d,5\%}$ [°C]	<sup>d)</sup> $E_y$ [MPa]	<sup>e)</sup> $\sigma$ [MPa]	<sup>f)</sup> $\epsilon_b$ [%]	<sup>g)</sup> $U_T$ [MJ m <sup>-3</sup> ]	<sup>h)</sup> Elastic recovery [%]
1-vinyl	0.00	-47	105*	309	1.0 ± 0.1	0.5 ± 0.02	1373 ± 93	4.7 ± 0.3	81
2-COOH	0.00	-51	100	287	9.0 ± 0.4	4.4 ± 0.1	2615 ± 175	88.4 ± 7.6	92
2-Na <sub>0.10</sub>	0.29	-50	91	285	18.8 ± 1.3	6.4 ± 0.4	610 ± 59	24.4 ± 3.4	78
2-Mg <sub>0.10</sub>	0.30	-51	80	290	11.5 ± 0.4	6.0 ± 0.3	996 ± 62	33.9 ± 2.1	88
2-Ca <sub>0.10</sub>	0.50	-51	82	290	13.2 ± 0.2	5.2 ± 0.7	790 ± 81	24.3 ± 4.8	88
2-Zn <sub>0.10</sub>	0.82	-51	86	275	11.8 ± 0.6	6.2 ± 0.6	1156 ± 87	37.7 ± 6.0	89
2-Al <sub>0.10</sub>	0.34	-54	136	273	51.5 ± 3.2	10.3 ± 0.3	361 ± 21	29.4 ± 2.2	99
2-Al <sub>0.05</sub>	0.17	-51	121	258	21.5 ± 1.0	9.6 ± 0.3	462 ± 24	30.8 ± 2.3	78
2-Al <sub>0.01</sub>	0.03	-50	100	270	12.4 ± 3.0	6.3 ± 0.4	630 ± 57	23.9 ± 3.0	82

<sup>a)</sup> Lower glass transition temperature from DSC; <sup>b)</sup> Upper glass transition temperature from peak in  $\tan(\delta)$  in DMTA, \*from DSC; <sup>c)</sup> Thermal degradation behavior is reported as the temperature at 5% mass loss, determined by TGA; <sup>d)</sup> Young's modulus; <sup>e)</sup> Tensile strength; <sup>f)</sup> Strain at break; <sup>g)</sup> Tensile toughness (area under the stress-strain curve). Mean values ± standard deviation from measurements conducted independently on 5 specimens; <sup>h)</sup> Elastic recovery determined from zero-force stress recovery experiment; materials were allowed to recover for 30 min from 0.3  $\epsilon_b$ .

result in some slight reductions in elongation at break, but samples are able to achieve strains in excess of 350%, which is certainly sufficient for many TPE applications.<sup>[27]</sup> The significant improvements in tensile strength and Young's modulus demonstrate the benefits of metal ion coordination and exemplify how a common starting polymer can be rapidly adjusted to meet specific material property demands (Figure 3c).

The elastic recovery was assessed by zero-force stress recovery experiments. Samples were strained to 30% of the elongation at break and allowed to freely recover for 30 min, i.e., under zero force/stress. Elastic recovery is the original length of the specimen relative to that after the 30 min recovery period (Table 2, Figure S55, Supporting Information). 2-COOH shows better elastic recovery, 92%, than the unfunctionalized polymer, likely because of dynamic inter-chain hydrogen bonding.<sup>[14b]</sup> All the ionomers show high elastic recovery values, with 2-Mg<sub>0.10</sub>, 2-Ca<sub>0.10</sub> and 2-Zn<sub>0.10</sub> being 88%–89%. The lead sample is, once again, 2-Al<sub>0.10</sub> that displays an impressive 99% elastic recovery. It is proposed that the Al(III) ions anchor the hard blocks and reduce chain pull-out, thereby driving efficient elastic recovery.<sup>[27b]</sup> In most applications, elastomers must also resist mechanical creep, or permanent deformation under applied stress.<sup>[28]</sup> To assess these aspects, rheological creep-recovery experiments were conducted using 1-vinyl, 2-COOH and 2-Al<sub>0.10</sub> (Figure 3d). The experiments were conducted at 30 °C, at a constant stress (5 kPa) for four periods of 100 s, each followed by 100 s of 0 Pa stress to recover. During the first cycle, 1-vinyl exhibited 11% strain that increased to 16% by the fourth cycle i.e., it showed significant creep. On the other hand, 2-COOH and 2-Al<sub>0.10</sub> only showed 2.0% and 0.9% strain, respectively, in the first cycles that did not increase in subsequent cycles. This excellent creep resistance is likely the result of improved hard-domain interactions.

Given the high tensile strength, elastic recovery, and creep resistance of the Al(III) ionomer, four different metal loadings were examined (as mol% metal vs carboxylic acid groups), targeting both lower (2-Al<sub>0.01</sub>, 2-Al<sub>0.05</sub>) and higher (2-Al<sub>0.12</sub> and 2-Al<sub>0.15</sub>) metal contents. The latter two samples (i.e., 12 and 15 mol%) were too densely cross-linked for subsequent processing either by solvent casting or compression moulding. On the other hand, 2-Al<sub>0.01</sub> and 2-Al<sub>0.05</sub> were both successfully processed into thin

films and uniaxial tensile testing allowed comparisons of Young's moduli, tensile strengths and strains at break of the ionomers (Figure 4a). The tensile strength correlates with the amount of Al(III) in the samples (0.03–0.34 wt%) and these experiments further demonstrate the potential tuning of tensile mechanical properties according to applications need.

To qualitatively investigate the influences of ionomer cross-link density, samples were subjected to solvent swelling experiments; in which lower swelling indices correlate with more strongly cross-linked networks. Uniform ionomer disks (8 mm diameter, ≈200 µm thick) were submerged in THF for 72 h, then dried (vacuum oven, 72 h) and weighed (both swollen and dried) to determine the swelling index and gel content respectively (Figure 4b and Table S4, Supporting Information). All ionomers showed high gel contents, from 92–99%, highlighting their chemical resistance. The swelling indices are highest for the metal(II) ionomers, indicating less effective cross-linking. In contrast, 2-Na<sub>0.10</sub> has a lower swelling index, consistent with the proposed sodium carboxylate aggregation. The lead sample, 2-Al<sub>0.10</sub> has the lowest swelling index and the highest cross-link density of all the materials. Further, as the Al(III) loading decreased, the swelling indices increased, consistent with reduced cross-linking (Figure 4b). Overall, the swelling indices of all the Al(III) samples are the lowest suggesting that even at very low loadings of Al(III) there is a maximized cross-link density. This notion is consistent with the tensile mechanical data, where 2-Al<sub>0.01</sub> has a greater tensile strength than the M(II) ionomers, even though it is applied at 1/10 the metal loading. This finding is significant since it allows for the highest mechanical strengths/Young's moduli using the lowest quantities of metal.

Given the promising performances of the Al(III) ionomers, their dynamic mechanical properties were investigated. All samples show wide-ranging rubbery plateau regions (Figure 4c). The plateau moduli of the Al(III) ionomers decrease with metal loading, particularly at elevated temperatures (34.3, 7.5 and 1.3 MPa at 120 °C for 2-Al<sub>0.10</sub>, 2-Al<sub>0.05</sub> and 2-Al<sub>0.01</sub> respectively). At Al(III) contents 5%–10%, the storage modulus is maintained to temperatures of 200 °C (which is well above the notional  $T_{g,upper}$ , Figure 4d) and the materials show a wide operating temperature range of –20–200 °C. It is proposed there is sufficient crosslink-

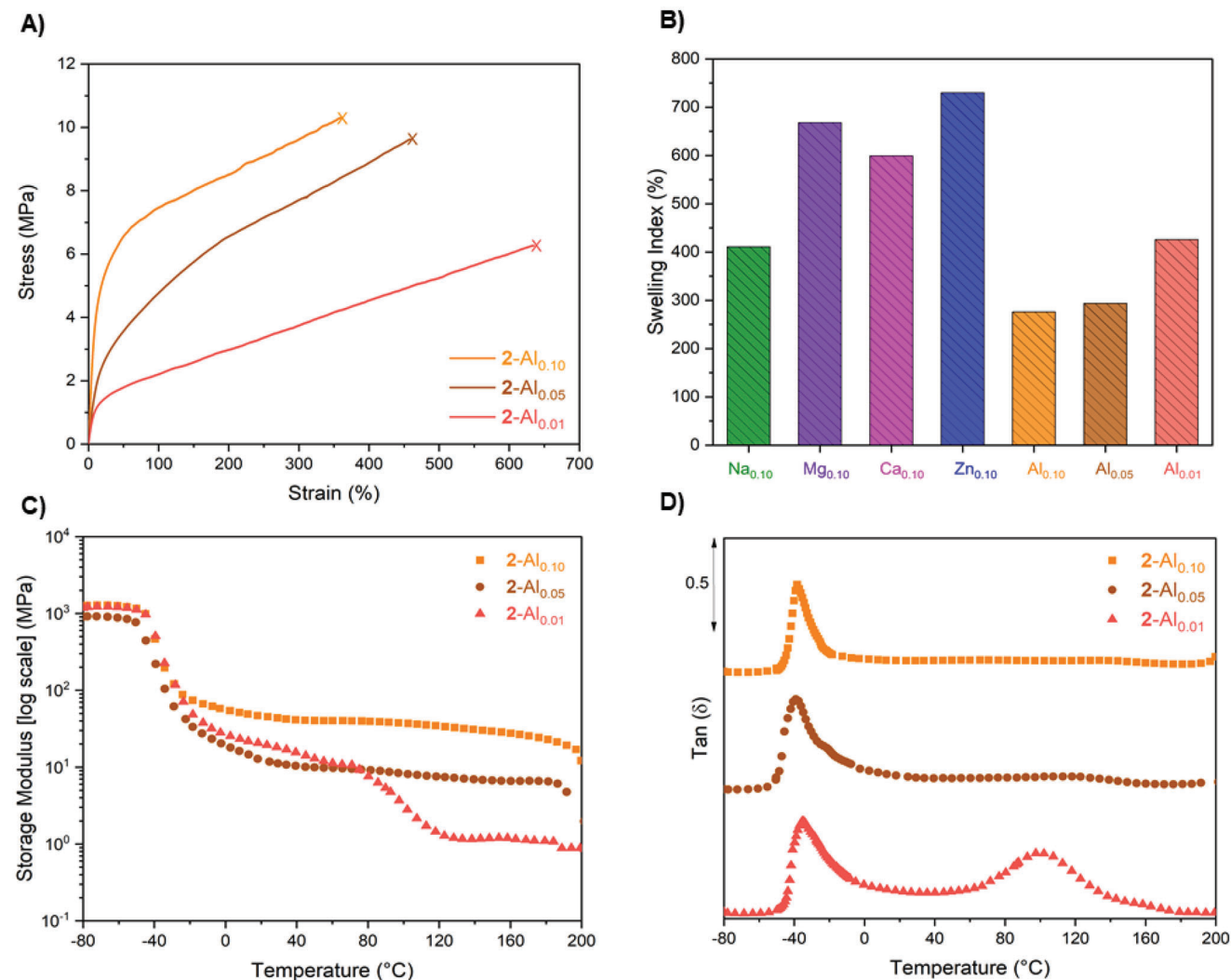


**Figure 4.** A) Representative stress–strain curves (10 mm min<sup>-1</sup> extension rate) for ionomers containing 10, 5 and 1 mol% aluminum. B) Swelling index after swelling polymer samples in THF for 72 h. C) Storage moduli and D) tan(δ) profiles from dynamic mechanical temperature analysis (DMTA) temperature sweeps of 2-Al<sub>0.10</sub>, 2-Al<sub>0.05</sub>, 2-Al<sub>0.01</sub>.

ing in 2-Al<sub>0.10</sub> and 2-Al<sub>0.05</sub> to restrict chain mobility. As a result, the upper glass transition temperature is raised and suppressed.

### 2.3. Polymer Recycling and Aqueous Stability Testing

Polymers designed to facilitate reprocessing could be advantageous in facilitating their end-of-life treatments since the energy required for mechanical recycling is usually significantly lower than for chemical recycling.<sup>[29]</sup> One advantage of these reversible chemical bonds should be their facility to undergo thermal reprocessing. Accordingly, the lead sample 2-Al<sub>0.01</sub> was successfully reprocessed three times, at 140 °C, without any compromise in thermal or mechanical properties (Figure S56, Supporting Information). This data show the potential to efficiently recycle both manufacturing scraps and even waste thermoplastic elastomer samples by simple heating protocols (above  $T_{g,upper}$ ) and without any material decomposition.

The aqueous stability of the polymers and ionomers was investigated by water swelling and base-catalyzed accelerated hydrolyses. For the aqueous swelling experiments, disks of 1-vinyl, 2-COOH and 2-Al<sub>0.10</sub> (16 mm diameter, ≈200 μm thick) were submerged in deionized water (pH = 7) and their swollen mass measured over time (Figure S57, Supporting Information). There were slight differences, with 2-COOH and 2-Al<sub>0.10</sub> showing increased water uptake but over 5 months no significant degradation occurred that is advantageous for any environmental exposure of products. To confirm the stability of the samples, the storage moduli were monitored as a function of the relative humidity using representative samples 1-vinyl, 2-COOH and 2-Al<sub>0.10</sub> (Figure S58, Supporting Information). All three materials maintained constant values for storage moduli from 0%–80% relative humidity demonstrating good stabilities over the duration of the experiments. Since the majority component of all samples is hydrophobic PDL, this prevents any compromise to sample mechanical integrity even in the most extreme of humid environ-



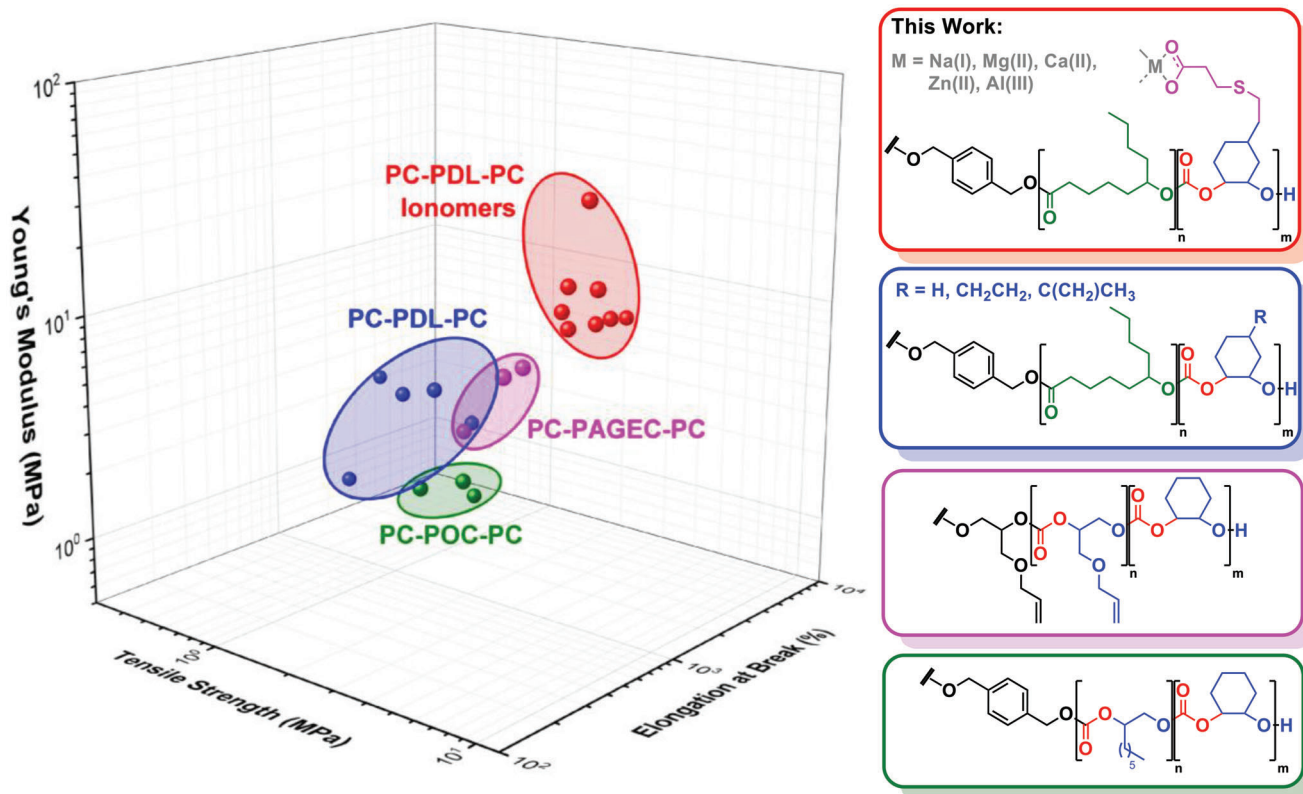


**Figure 5.** Ashby plot for literature CO<sub>2</sub>-polymer thermoplastic elastomers and CO<sub>2</sub>-polymer ionomers (this work). PC = polycarbonate, PDL = poly( $\epsilon$ -decalactone), PAGEC = poly(allyl glycidyl ether carbonate),<sup>[9a]</sup> and POC = poly(octene carbonate).<sup>[9b]</sup> PC-PDL-PC are ABA triblock copolymers with PDL B-blocks and CO<sub>2</sub>/epoxide (cyclohexene oxide, 4-vinyl-cyclohexene oxide and limonene oxide) A blocks.<sup>[11i,16]</sup>

ments. Finally, accelerated aging experiments were conducted using a strong base. Accordingly, disks of 1-vinyl, 2-COOH and 2-Al<sub>0.10</sub> (16 mm diameter,  $\approx 200$   $\mu$ m thick) were submerged in 1 M NaOH solutions at room temperature and mass loss over time was measured (Figure S59, Supporting Information). The Al(III) ionomer, 2-Al<sub>0.10</sub>, showed significantly faster hydrolysis compared to 1-vinyl or 2-COOH, achieving 50% mass loss over 5 months. In future these accelerated hydrolyses could be exploited and accelerated, e.g., with higher temperatures, in future for chemical recycling.

### 3. Discussion

The ABA block polymers are derived from CO<sub>2</sub>, a common waste product abundant as a co-product of chemical/bio-chemical manufacturing, and  $\epsilon$ -decalactone, sourced from castor oil via ricinoleic acid.<sup>[30]</sup> As such, these polymers comprise  $\approx 75$  wt% renewable resources and using efficient chemistry, simple carboxylic acid substituents were installed at regular sites through the polycarbonate “hard” blocks. These carboxylic acid groups coordinate metals including Na(I), Mg(II), Ca(II), Zn(II) and Al(III) to make new ionomer elastomers. The overall metal loadings were very low in all samples,  $<1$  wt%, allowing for optical transparency, but despite these low loadings, the nature of the metal, and specifically its oxidation state or valency controls the polymers’ thermal and mechanical properties. In particular, the greatest tensile strengths were afforded by low quantities

of Al(III) and the products combined broad operating temperatures with high upper service temperatures ( $-20$ – $200$   $^{\circ}$ C). The latter temperature compares favorably with TPE featuring PLA ( $\approx 60$   $^{\circ}$ C),<sup>[31]</sup> polystyrene ( $\approx 100$   $^{\circ}$ C),<sup>[27a]</sup> or poly(cyclohexene-*alt*-phthalate) ( $\approx 120$   $^{\circ}$ C) hard blocks.<sup>[14a]</sup> There are significant benefits to using low quantities of metals to increase tensile mechanical strengths and toughness, without compromising elastic recovery and with minimal creep. Further, the elastomers can be reprocessed thermally that should help future recycling. There are three areas of novelty or property moderation that are worth more detailed contextualization versus the literature.

The first is the distinct improvements to the properties of carbon-dioxide-derived polymers (PC) afforded by the metal carboxylates. These new polymers ( $\approx 5$  wt% CO<sub>2</sub>) reach previously inaccessible regions of property space compared with other CO<sub>2</sub>-derived polymer elastomers (Figure 5). Compared with other elastomers featuring the same polyester “soft” block (i.e., PDL), the ionomers showed significant increases to all tensile mechanical properties, i.e., they performed better than equivalent materials using poly(cyclohexene carbonate), poly(vinyl-cyclohexene carbonate) or poly(limonene carbonate) “hard blocks”.<sup>[11i,16]</sup> Further the increases in tensile strength do not compromise elasticity, with materials showing high elastic recovery and high creep-resistance. The new polymers also improved upon prior reported carbon-dioxide-derived polycarbonate elastomers. Compared with materials featuring “soft blocks” such as poly(allyl glycidyl ether carbonate) (PAGEC) or poly(octene carbonate) (POC),

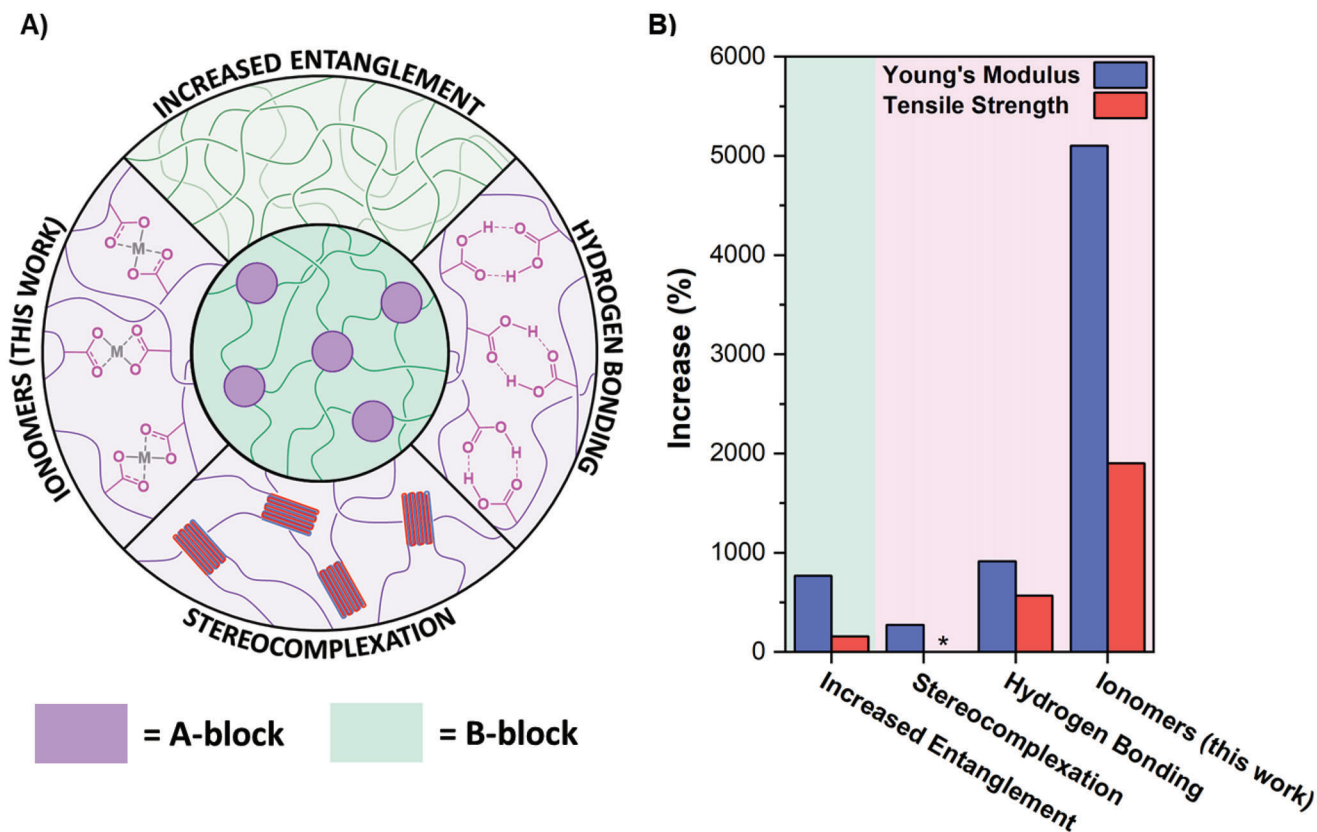


**Figure 6.** A) Schematic representation of various approaches to increase mechanical properties of TPEs. B) The resulting improvements in Young's modulus and tensile strengths relative to unfunctionalized material (Table S5, Supporting Information). \*No increase.

these ionic elastomers showed over 50% and 200% higher tensile strengths and over 400% and 1900% higher Young's moduli, respectively, and maintained the same poly(cyclohexene carbonate) hard blocks.<sup>[9]</sup> Since the production of the current materials was highly controlled, there are many future options to combine different lactones, epoxides or heterocumulenes to fine-tune properties. If higher bio-based content is desired, a hard-block polymer comprising limonene oxide (LO) and carbon dioxide could be targeted, since both its catalysis and "hard block" properties are benchmarked.<sup>[11]</sup> The step-changes in mechanical performances afforded by these ABA block polymers, compared with the current state-of-the-art polymers, offer significant scope for future property explorations and expand the range and application potential for carbon-dioxide-derived plastics.

The second feature is the facility to "tune" properties without requiring any polymer backbone re-design or changes to processing conditions. This aspect is significant since prior solutions to these challenges generally involved new monomers and polymers. While appropriate in academic discovery, there could be some disadvantages to moderating properties through changes to monomer chemistry since for every new product the monomer syntheses, polymerization catalysts and conditions must be (re)optimized. There are also several known approaches to increasing elastomer tensile strengths and comparably metal ion coordination appears promising. One excellent approach has been to increase the soft-block entanglement by using B-block polymers showing low entanglement molar mass ( $M_e$ ). This

strategy has resulted in  $\approx 770\%$  increases in Young's modulus and  $\approx 150\%$  increase in tensile strength (compared with equivalent polymers applying soft blocks with higher  $M_e$ ).<sup>[13d]</sup> Alternatively, the hard-blocks can be reinforced by (co-)crystallization, for example by PLLA/PDLA stereo-complexation, which achieved  $\approx 270\%$  higher Young's modulus but did little to change the overall tensile strength (compared with PLLA materials alone).<sup>[32]</sup> Despite the undoubted successes of the prior approaches, installing metal complexes allows for greater increases in properties showing  $\approx 1900\%$  in tensile strengths and  $\approx 5100\%$  in Young's moduli (Figure 6). Given the magnitude of the increment is controlled by the quantity of the added metal, it's easily feasible to moderate properties over a very wide range of values.

Finally, the metal ion coordination strategy should be practically achievable, and this work has deliberately focused on precision structures using commercial monomers combined with low-cost, colorless, and Earth-abundant metals to improve future sustainability and applicability. Materials were prepared using controlled switchable polymerizations, combining commercial lactone ROP and epoxide/carbon dioxide ROCOP, with a single catalyst. The precision block polymer structures allow for high control and regulation over both the extent and site of metal ion coordination and subsequent properties. In future, a range of different coordination chemistries should be explored to provide an understanding of the relationships between inorganic macromolecular chemistry and macroscopic properties.

## 4. Conclusions

Installing metal-carboxylate bonds within the hard domains of CO<sub>2</sub>- and bio-derived triblock copolymer thermoplastic elastomers allowed for control over and improvements to tensile mechanical properties. Materials were prepared with <1 wt% metal yet showed significantly higher tensile strengths and toughness, while maintaining high elasticity, elastic recovery, and creep resistance. Well-controlled polymer syntheses ensured regular placement of coordination sites along the chain, allowing for accurate control over the cross-linking density and tuning the thermal and mechanical properties. Using <1 wt% aluminum in the polymers resulted in a 52-fold increase in the material's Young's modulus and a 21-fold increase in tensile strength relative to the starting polymer. The ionomer polymers showed wide operating (−20 to 200 °C) and processing temperature ranges (150–250 °C); materials were also recyclable by compression moulding and showed good environmental stability. This new chemistry should be applicable to many other monomer combinations, polymer structures and metal–ligand coordination chemistries providing an exciting array of future materials and mechanisms for property tuning. In future sustainable polymers need to show a wide variety of properties to replace current petrochemical plastics and elastics.

## Supporting Information

Supporting Information is available from the Wiley Online Library or from the author.

## Acknowledgements

The EPSRC (EP/S018603/1; EP/R027129/1; EP/V003321/1), Oxford Inorganic Chemistry for Future Manufacturing Centre for Doctoral Training (EP/S023828/1), Research England (RED, RE-P-2020-04), The Oxford Martin School (Future of Plastics) and the Faraday Institution (SOLBAT, FIRG-007, FIRG056) are acknowledged for research funding. The Diamond Light Source and Dr. Nicholas Terrill and Dr. Sam Burholt are sincerely thanked for Rapid Access DL-SAXS measurements (SM2617-1).

## Conflict of Interest

The authors declare no conflict of interest.

## Data Availability Statement

The data that support the findings of this study are available from the corresponding author upon reasonable request.

## Keywords

bio-derived materials, carbon dioxide, epoxide, ionomers, lactone, polycarbonate, polyester, ring-opening copolymerization, ring-opening polymerization, thermoplastic elastomers

Received: March 27, 2023  
Revised: May 4, 2023  
Published online: July 23, 2023

- [1] a) Y. Q. Zhu, C. Romain, C. K. Williams, *Nature* **2016**, *540*, 354; b) D. K. Schneiderman, M. A. Hillmyer, *Macromolecules* **2017**, *50*, 3733.
- [2] a) J. J. Zheng, S. Suh, *Nat. Clim. Change* **2019**, *9*, 567; b) A. Singh, N. A. Rorrer, S. R. Nicholson, E. Erickson, J. S. DesVeaux, A. F. T. Avelino, P. Lamers, A. Bhatt, Y. M. Zhang, G. Avery, L. Tao, A. R. Pickford, A. C. Carpenter, J. E. McGeehan, G. T. Beckham, *Joule* **2021**, *5*, 2479.
- [3] F. M. Haque, J. S. A. Ishibashi, C. A. L. Lidston, H. L. Shao, F. S. Bates, A. B. Chang, G. W. Coates, C. J. Cramer, P. J. Dauenhauer, W. R. Dichtel, C. J. Ellison, E. A. Gormong, L. S. Hamachi, T. R. Hoyer, M. Y. Jin, J. A. Kalow, H. J. Kim, G. Kumar, C. J. LaSalle, S. Liffland, B. M. Lipinski, Y. T. Pang, R. Parveen, X. Y. Peng, Y. Popowski, E. A. Prebhalo, Y. Reddi, T. M. Reineke, D. T. Sheppard, J. L. Swartz, et al., *Chem. Rev.* **2022**, *122*, 6322.
- [4] a) G. W. Coates, Y. D. Y. L. Getzler, *Nat. Rev. Mater.* **2020**, *5*, 501; b) M. Hong, E. Y. X. Chen, *Green. Chem.* **2017**, *19*, 3692.
- [5] X. Y. Zhang, M. Fevre, G. O. Jones, R. M. Waymouth, *Chem. Rev.* **2018**, *118*, 839.
- [6] a) C. Hepburn, E. Adlen, J. Beddington, E. A. Carter, S. Fuss, N. M. Dowell, J. C. Minx, P. Smith, C. K. Williams, *Nature* **2019**, *575*, 87; b) Y. Y. Zhang, G. P. Wu, D. J. Darensbourg, *Trends Chem.* **2020**, *2*, 750.
- [7] a) N. von der Assen, J. Jung, A. Bardow, *Environ. Sci.* **2013**, *6*, 2721; b) N. von der Assen, A. Bardow, *Green. Chem.* **2014**, *16*, 3272; c) J. Artz, T. E. Muller, K. Thenert, J. Kleinekorte, R. Meys, A. Sternberg, A. Bardow, W. Leitner, *Chem. Rev.* **2018**, *118*, 434.
- [8] a) J. Langanke, A. Wolf, J. Hofmann, K. Bohm, M. A. Subhani, T. E. Muller, W. Leitner, C. Gurtler, *Green. Chem.* **2014**, *16*, 1865; b) M. Scharfenberg, J. Hilf, H. Frey, *Adv. Funct. Mater.* **2018**, *28*, 1704302; c) T. Stosser, C. L. Li, J. Unruangsri, P. K. Saini, R. J. Sablong, M. A. R. Meier, C. K. Williams, C. Koning, *Polym. Chem.* **2017**, *8*, 6099; d) P. Alagi, R. Ghorpade, Y. J. Choi, U. Patil, I. Kim, J. H. Baik, S. C. Hong, *ACS Sustainable Chem. Eng.* **2017**, *5*, 3871; e) O. Hauenstein, S. Agarwal, A. Greiner, *Nat. Commun.* **2016**, *7*, 11862; f) M. DeBolt, A. Kiziltas, D. Mielewski, S. Waddington, M. J. Nagridge, *J. Appl. Polym. Sci.* **2016**, *133*, <https://doi.org/10.1002/app.44086>; g) S. H. Lee, A. Cyriac, J. Y. Jeon, B. Y. Lee, *Polym. Chem.* **2012**, *3*, 1215.
- [9] a) G. W. Yang, G. P. Wu, *ACS Sustainable Chem. Eng.* **2019**, *7*, 1372; b) M. C. Jia, D. Y. Zhang, G. W. de Kort, C. H. R. M. Wilsens, S. Rastogi, N. Hadjichristidis, Y. Gnanou, X. S. Feng, *Macromolecules* **2020**, *53*, 5297.
- [10] a) C. Koning, J. Wildeson, R. Parton, B. Plum, P. Steeman, D. J. Darensbourg, *Polymer* **2001**, *42*, 3995; b) O. Hauenstein, M. Reiter, S. Agarwal, B. Rieger, A. Greiner, *Green. Chem.* **2016**, *18*, 760; c) S. D. Thorat, P. J. Phillips, V. Semenov, A. Gakh, *J. Appl. Polym. Sci.* **2003**, *89*, 1163; d) Y. Y. Wang, D. J. Darensbourg, *Coord. Chem. Rev.* **2018**, *372*, 85.
- [11] a) F. N. Singer, A. C. Deacy, T. M. McGuire, C. K. Williams, A. Buchard, *Angew. Chem., Int. Ed.* **2022**, *61*, e202201785; b) T. M. McGuire, A. C. Deacy, A. Buchard, C. K. Williams, *J. Am. Chem. Soc.* **2022**, *144*, 18444; c) Y. Liu, H. Zhou, J. Z. Guo, W. M. Ren, X. B. Lu, *Angew. Chem., Int. Ed.* **2017**, *56*, 4862; d) Y. Yu, L. M. Fang, Y. Liu, X. B. Lu, *ACS Catal.* **2021**, *11*, 8349; e) Y. Yu, B. Gao, Y. Liu, X. B. Lu, *Angew. Chem., Int. Ed.* **2022**, *61*, e202204492; f) D. J. Darensbourg, S. H. Wei, A. D. Yeung, W. C. Ellis, *Macromolecules* **2013**, *46*, 5850; g) D. J. Darensbourg, A. D. Yeung, S. H. Wei, *Green. Chem.* **2013**, *15*, 1578; h) C. L. Li, R. J. Sablong, R. A. T. M. van Benthem, C. E. Koning, *ACS Macro Lett* **2017**, *6*, 684; i) L. P. Carrodegua, T. T. D. Chen, G. L. Gregory, G. S. Sulley, C. K. Williams, *Green. Chem.* **2020**, *22*, 8298; j) G. W. Yang, Y. H. Wang, H. Qi, Y. Y. Zhang, X. F. Zhu, C. J. Lu, L. Yang, G. P. Wu, *Angew. Chem., Int. Ed.* **2022**, *61*, e202210243.
- [12] W. Y. Wang, W. Lu, A. Goodwin, H. Q. Wang, P. C. Yin, N. G. Kang, K. L. Hong, J. W. Mays, *Prog. Polym. Sci.* **2019**, *95*, 1.
- [13] a) M. A. Hillmyer, W. B. Tolman, *Acc. Chem. Res.* **2014**, *47*, 2390; b) D. K. Schneiderman, M. A. Hillmyer, *Macromolecules* **2016**, *49*, 2419; c) M. T. Martello, M. A. Hillmyer, *Macromolecules* **2011**, *44*,

- 8537; d) A. Watts, N. Kurokawa, M. A. Hillmyer, *Biomacromolecules* **2017**, *18*, 1845; e) M. T. Martello, D. K. Schneiderman, M. A. Hillmyer, *ACS Sustainable Chem. Eng.* **2014**, *2*, 2519; f) P. Olsen, T. Borke, K. Odelius, A. C. Albertsson, *Biomacromolecules* **2013**, *14*, 2883.
- [14] a) G. L. Gregory, G. S. Sulley, L. P. Carrodegua, T. T. D. Chen, A. Santmarti, N. J. Terrill, K. Y. Lee, C. K. Williams, *Chem. Sci.* **2020**, *11*, 6567; b) G. L. Gregory, C. K. Williams, *Macromolecules* **2022**, *55*, 2290; c) G. L. Gregory, G. S. Sulley, J. Kimpel, M. Lagodzinska, L. Hafele, L. P. Carrodegua, C. K. Williams, *Angew. Chem., Int. Ed.* **2022**, *61*, e202210748.
- [15] a) A. C. Deacy, G. L. Gregory, G. S. Sulley, T. T. D. Chen, C. K. Williams, *J. Am. Chem. Soc.* **2021**, *143*, 10021; b) Y. Y. Zhang, G. W. Yang, R. Xie, X. F. Zhu, G. P. Wu, *J. Am. Chem. Soc.* **2022**, *144*, 19896.
- [16] G. S. Sulley, G. L. Gregory, T. T. D. Chen, L. P. Carrodegua, G. Trott, A. Santmarti, K. Y. Lee, N. J. Terrill, C. K. Williams, *J. Am. Chem. Soc.* **2020**, *142*, 4367.
- [17] J. K. Zhao, G. W. Yang, X. F. Zhu, G. P. Wu, *Polym. Chem.* **2019**, *10*, 5265.
- [18] E. Degtyar, M. J. Harrington, Y. Politi, P. Fratzl, *Angew. Chem., Int. Ed.* **2014**, *53*, 12026.
- [19] J. E. Hillerton, J. F. V. Vincent, *J. Exp. Biol.* **1982**, *101*, 333.
- [20] G. E. Fantner, T. Hassenkam, J. H. Kindt, J. C. Weaver, H. Birkedal, L. Pechenik, J. A. Cutroni, G. A. G. Cidade, G. D. Stucky, D. E. Morse, P. K. Hansma, *Nat. Mater.* **2005**, *4*, 612.
- [21] a) X. H. Zhao, X. Y. Chen, H. Yuk, S. T. Lin, X. Y. Liu, G. Parada, *Chem. Rev.* **2021**, *121*, 4309; b) Z. C. Wei, H. Y. Duan, G. S. Weng, J. He, *J. Mater. Chem.* **2020**, *8*, 15956; c) D. Mozhdehi, S. Ayala, O. R. Cromwell, Z. B. Guan, *J. Am. Chem. Soc.* **2014**, *136*, 16128; d) C. M. Brown, D. J. Lundberg, J. R. Lamb, I. Kevlishvili, D. Kleinschmidt, Y. S. Alfaraj, H. J. Kulik, M. F. Ottaviani, N. J. Oldenhuis, J. A. Johnson, *J. Am. Chem. Soc.* **2022**, *144*, 13276.
- [22] a) M. O. M. Piepenbrock, G. O. Lloyd, N. Clarke, J. W. Steed, *Chem. Rev.* **2010**, *110*, 1960; b) S. C. Grindy, R. Learsch, D. Mozhdehi, J. Cheng, D. G. Barrett, Z. B. Guan, P. B. Messersmith, N. Holten-Andersen, *Nat. Mater.* **2015**, *14*, 1210; c) C. Creton, *Macromolecules* **2017**, *50*, 8297.
- [23] a) J. E. Potaufoux, J. Odent, D. Notta-Cuvier, F. Lauro, J. M. Raquez, *Polym. Chem.* **2020**, *11*, 5914; b) E. Khare, N. Holten-Andersen, M. J. Buehler, *Nat. Rev. Mater.* **2021**, *6*, 421; c) W. T. Wang, J. Zhang, F. Jiang, X. H. Wang, Z. G. Wang, *ACS Appl Polym Mater* **2019**, *1*, 571; d) C. H. Li, C. Wang, C. Keplinger, J. L. Zuo, L. Jin, Y. Sun, P. Zheng, Y. Cao, F. Lissel, C. Linder, X. Z. You, Z. A. Bao, *Nat. Chem.* **2016**, *8*, 619; e) J. C. Lai, L. Li, D. P. Wang, M. H. Zhang, S. R. Mo, X. Wang, K. Y. Zeng, C. H. Li, Q. Jiang, X. Z. You, J. L. Zuo, *Nat. Commun.* **2018**, *9*, 2725; f) Y. Miwa, J. Kurachi, Y. Kohbara, S. Kutsumizu, *Commun. Chem.* **2018**, *1*, 5.
- [24] E. Filippidi, T. R. Cristiani, C. D. Eisenbach, J. H. Waite, J. N. Israelachvili, B. K. Ahn, M. T. Valentine, *Science* **2017**, *358*, 502.
- [25] A. Spyros, D. S. Argyropoulos, R. H. Marchessault, *Macromolecules* **1997**, *30*, 327.
- [26] a) T. Kajita, H. Tanaka, A. Noro, Y. Matsushita, A. Nozawa, K. Isobe, R. Oda, S. Hashimoto, *Polymer* **2021**, *217*, 123419; b) V. Otero, D. Sanches, C. Montagner, M. Vilarigues, L. Carlyle, J. A. Lopes, M. J. Melo, *J. Raman Spectrosc.* **2014**, *45*, 1197.
- [27] a) J. G. Drobný, *Handbook of Thermoplastic Elastomers*, 2nd ed., **2014**; b) M. J. Fasolka, A. M. Mayes, *Ann. Rev. Mater. Res.* **2001**, *31*, 323.
- [28] R. W. Clarke, M. L. McGraw, B. S. Newell, E. Y. X. Chen, *Cell Rep. Phys. Sci.* **2021**, *2*, 100483.
- [29] a) V. Piemonte, S. Sabatini, F. Gironi, *J. Polym. Environ.* **2013**, *21*, 640; b) M. F. C. de Andrade, P. M. S. Souza, O. Cavalett, A. R. Morales, *J. Polym. Environ.* **2016**, *24*, 372.
- [30] a) A. M. Chapman, C. Keyworth, M. R. Kember, A. J. J. Lennox, C. K. Williams, *ACS Catal.* **2015**, *5*, 1581; b) Y. Q. Zhu, M. R. Radlauer, D. K. Schneiderman, M. S. P. Shaffer, M. A. Hillmyer, C. K. Williams, *Macromolecules* **2018**, *51*, 2466.
- [31] V. Arias, A. Hoglund, K. Odelius, A. C. Albertsson, *Biomacromolecules* **2014**, *15*, 391.
- [32] C. L. Wanamaker, M. J. Bluemle, L. M. Pitet, L. E. O'Leary, W. B. Tolman, M. A. Hillmyer, *Biomacromolecules* **2009**, *10*, 2904.